

Biofabrication of silver nanoparticles using *Curcuma longa* extract: Effects of extraction and synthesis conditions, characteristics, and its antibacterial activity

Nguyen D. Trung, Nguyen T. Nhuan, Luong T. C. Van, Nguyen V. Minh, Nguyen P. Anh, and Nguyen Tri*

Received: 08 July 2019 / Received in revised form: 26 December 2019, Accepted: 08 January 2020, Published online: 28 February 2020
© Biochemical Technology Society 2014-2020
© Sevas Educational Society 2008

Abstract

This investigation was done to synthesize silver nanoparticles (AgNPs) using *Curcuma longa* (*C. longa*) extract as a capping, and stabilizing, reducing agent. The impact of *C. longa* raw material/water ratio, extraction duration and temperature, the volume ratios of AgNO₃ solution/*C. longa* extract, and AgNO₃ concentration in the formation of AgNPs were evaluated. The obtained AgNPs were analyzed by UV-Vis spectroscopy, FTIR, X-ray diffraction pattern (XRD), energy-dispersive X-ray spectroscopy (EDX), transmission electron microscopy (TEM), and the size distribution estimated by zeta instrument. The presence of AgNPs exhibited surface plasmon resonance peak approximately at 442 nm. FTIR study demonstrated that hydroxyl functional groups existed in the extract that reduced Ag⁺ to Ag⁰. XRD pattern was used to identify the crystalline structure of AgNPs. The morphology and size of the synthesized AgNPs were determined by TEM. The obtained AgNPs with a face-centered

cubic structure were nearly spherical in shape and 5–30 nm in diameter, and the average size of particles was 28.0 nm. The antibacterial activity of AgNPs was investigated against *Bacillus cereus* (*B. cereus*), *Escherichia coli* (*E. coli*), *Staphylococcus aureus* (*S. aureus*), and *Salmonella typhi* (*Salmonella*) by disc diffusion method. The inhibition zone of obtained AgNPs against bacteria varied in a range of 15–20 mm and the minimum inhibitory concentrations were determined only 2.81 – 11.5 µg.ml⁻¹.

Key words: Biofabrication, silver nanoparticles, *Curcuma longa*, synthesis conditions, antibacterial activity

Introduction

Silver nanoparticles (AgNPs) have been used in different fields such as environmental pollution, drug delivery, and materials because of the exclusive characteristics (Gittins et al., 2000). Chemical synthesis of AgNPs requires hazardous reducing agents to convert Ag⁺ ions into Ag⁰ nanoparticles (Mukherjee et al., 2008). By contrast, the green synthesis using eco-friendly reducing reagents had effective cost and was manufactured with a large scale (Sandeep et al., 2016). In the biosynthesis method, various extracts are used as reducing, stabilizing, and capping agents for AgNPs formation (Krithiga and Briget, 2015). Phytochemicals present in extracts including alkaloids, flavonoids, terpenoids, amino acids, tannins, saponins, phenols, and carbohydrates act as agents for the biosynthesis of AgNPs (PANDIT, 2015; Janeeta Priya et al., 2016).

Curcuma longa (*C. longa*) is a medicinal plant that belongs to the Zingiberaceae (ginger family) and widely grown in subtropical and tropical climate (Prasad et al., 2014). It is considered as a source of bioactive compounds including glycosides, sterols, alkaloids, flavonoids, and saponins (Abraham et al., 2018). Curcumin is known as an orange-yellow colored polyphenol and constitutes *C. longa* powder. Studies have been determined that curcumin has antimutagenic, antiangiogenic, anti-inflammatory, antimicrobial, antioxidant, and antiplatelet aggregation activity (Patil et al., 2009; Shehzad et al., 2013). To the best of the authors' knowledge and understanding, most of the previous studies only evaluated the effect of factors on the AgNPs formation from *C. longa* powder and antibacterial activity of the synthesized AgNPs.

Nguyen D. Trung

School of Education, Can Tho University, 94000, Vietnam.
Graduate University of Science and Technology, Vietnam
Academy of Science and Technology, 100000, Vietnam.

Nguyen T. Nhuan

School of Education, Can Tho University, 94000, Vietnam.

Luong T. C. Van, Nguyen V. Minh

Biotechnology Department, Ho Chi Minh City Open
University, 700000, Vietnam.

Nguyen P. Anh

Graduate University of Science and Technology, Vietnam
Academy of Science and Technology, 100000, Vietnam.
Institute of Chemical Technology, Vietnam Academy of
Science and Technology, 700000, Vietnam.

Nguyen Tri*

Biotechnology Department, Ho Chi Minh City Open
University, 700000, Vietnam.
Institute of Chemical Technology, Vietnam Academy of
Science and Technology, 700000, Vietnam

*Email: ntri @ ict.vast.vn

According to previous publications, Shamel et al. (2012) synthesized AgNPs from aqueous AgNO₃ using *C. longa* tuber-powder extract as a reductant agent. TEM images showed that the average particle size for the formation of AgNPs was 6.30 ± 2.64 nm. XRD showed a face-centered cubic structure of AgNPs with high crystalline. Another study in the synthesis of AgNPs using *C. longa* extract was done by Manonmani et al. (2015). The antibacterial effect of AgNPs was tested against *E. coli*, *Pseudomonas sp.*, *Salmonella sp.*, *Bacillus sp.*, and *Staphylococcus sp.* In *E. coli*, the inhibition zone was a maximum of 25 mm. Meanwhile, AgNPs showed an inhibition zone of 23, 22, 24, and 24 mm for *Salmonella sp.*, *Pseudomonas sp.*, *Bacillus sp.*, and *Staphylococcus sp.*, respectively. AgNPs prepared from silver sulfate solution using *Curcuma Longa* also were studied by Kurian et al. (2016). TEM images determined the presence of AgNPs with sizes of 20–50 nm. The antibacterial studies of the AgNPs were determined using the Agar well diffusion assay method against *Staphylococcus aureus*. The inhibition zone was observed at 14 mm for 1mM Ag and 16 mm for 5 mM Ag. So, it demonstrated that the use of *C. longa* extract as a combined stabilizing and reducing agent is an efficient and promising methods in the preparation of AgNPs. Although there are also numerous studies on the synthesis of AgNPs utilizing *C. longa* extract, they are not systematic and comprehensive, especially in the antibacterial activities as well as the mechanism of the formation of AgNPs using *C. longa* extract as a combined stabilizing and reducing agent. Meanwhile, the effect of extraction condition had not been mentioned (Shamel et al., 2012; Garg and Garg, 2018; Sathishkumar et al., 2010; Yang et al., 2016).

In this work, AgNPs were synthesized by the reduction of AgNO₃ solution using *C. longa* extract. The effect of *C. longa* extraction including raw material/water ratio, extraction duration and temperature, the volume ratios of AgNO₃ solution/*C. longa* extract, and AgNO₃ concentration in the formation of AgNPs were evaluated. The characterization of obtained AgNPs was done and its antibacterial activity was evaluated against bacteria: *B. cereus*, *E. coli*, *S. aureus*, and *Salmonella*. Furthermore, the antibacterial effect of the synthesized AgNPs against *S. aureus* was studied on gauze pads.

Materials and Methods

Silver nitrate (AgNO₃, Merck), and distilled water were used in this study. The *C. longa* tubers were collected and washed several times with distilled water to eliminate the dust particles, cut into small pieces, dried at 40 °C within 24 h, and then ground to a fine powder (the particle size < 0.25 mm). The obtained powder was used for further studies.

C. longa powder (x grams) was dispersed in 1 L of distilled water. The mixture was boiled at T °C for t min to extract reducing agents in the presence of *C. longa* powder. The experiments were performed at different temperatures (T = 40, 50, 60, and 70 °C) and various durations (t = 5, 10, 15, 25, and 45 min) For evaluating the effect of duration and temperature on *C.*

longa extraction. The extract was cooled to room temperature, then filtered through a Whatman filter paper (2.5 µm) and centrifuged at 5000 rpm for 30 min to get rid of the heavy biomaterials. The extract was stored at 4 °C in order to be used for further experiments.

For AgNPs synthesis, the precursor of silver was used as being AgNO₃ solution in distilled water. A typical reaction mixture containing V_{ext} ml of extract in V_{Ag+} ml of C_{Ag+} mM AgNO₃ solution was prepared. The synthesis was performed at room temperature for 90 min with continuous stirring.

The effect of the ratio of *C. longa* raw material and distilled water on the AgNPs synthesis was determined by adding different amounts of the powered *C. longa* (5.0, 7.5, 10.0, and 12.5 g). Moreover, the effect of V_{Ag+}/V_{ext} ratio on AgNPs synthesis was determined by alteration V_{Ag+}/V_{ext} = 1, 2, 3, and 4. Finally, the effect of the concentration of AgNO₃ on the preparation of AgNPs was studied at C_{Ag+} = 1.00, 1.25, 1.50, and 1.75 mM.

The presence of synthesized AgNPs in the solution was determined by UV-Vis spectrophotometer (UV-1800, Shimadzu) in the range of 300–700 nm. The crystalline structure of the synthesized AgNPs powder dried at 60 °C under vacuum pressure (–700 mmHg) within 12 h was confirmed by XRD (Bruker D2 Phaser X-Ray Diffractometer, Bruker) with Cu Kα radiation (40 mA, 40 kV) and the scanning step of 0.02°. The FTIR spectra were measured using Bruker Tensor 2700 FTIR spectrometer operated in the range of 400–4,000 cm⁻¹ with a resolution of 4 cm⁻¹ using thin transparent KBr pellets to characterize the functional groups of synthesized AgNPs. EDX (JED-2300, Akishima) was used for the elemental analysis of the synthesized nanoparticles. The morphology and size of AgNPs were determined by TEM (JEOL 1400). The size distribution of AgNPs was estimated by the zeta instrument (Zetasizer, Malvern).

The synthesized AgNPs were tested for antibacterial effect against *E.coli* ATCC 25922, *B. cereus* ATCC 14579, *S. aureus* ATCC 43300 (MRSA), and *Salmonella* ATCC 14028 using an agar well diffusion method. Pre-cultivation of the bacteria was conducted on nutrient agar slant at 37 °C in 24 h by pricking a single colony of each of the microbial strains, and the bacteria were then diluted the cultures from slants in 0.85% NaCl with a density equivalent to 0.5 McFarland standard (1.5×10⁸ CFU/mL⁻¹) to prepare the inoculum of each strain. After the preparation of the Muller Hinton Agar plates, four 6mm-wells were made on each plate. 70 µl of synthesized AgNPs solution was added to three out of the four wells on each plate. The remaining one was used as the control. After 15min for AgNPs to diffuse into the agar, the samples were incubated at 37 °C for 24h. Finally, the results were recorded by measuring the diameter of the inhibition zone around the agar. To examine the minimum inhibitory concentration of AgNPs against four bacteria, different concentrations of AgNPs (N/2, N/4, N/8, N/16, N/32, and N/64 with N was the initial concentration of 90 µg/mL⁻¹) were prepared by diluting AgNPs solution with deionized water. The lowest

concentration of AgNPs that inhibited the growth of tested bacteria was considered as the MIC.

Results and Discussion

Effects of *C. longa* extraction conditions

Figure 1 shows the effect of extraction condition on the synthesis of AgNPs. As can be seen, the content of *C. longa* powder plays a vital role to form AgNPs. To determine the effect of *C. longa* powder content on the formation of AgNPs, the samples were prepared by the addition of different concentrations of powder (5.0, 7.5, 10.0, and 12.5 g.L⁻¹) into the reaction solutions with the AgNO₃ solution (1.0 mM)/*C. longa* extract volume ratio of 2 at room temperature for 90 min. Figure 1a shows the AgNPs formation with different *C. longa* powder contents from 5.0 to 12.5 g.L⁻¹. The low concentration of AgNPs was produced at *C. longa* powder concentration of 5.0 and 7.5 g.L⁻¹ due to insufficient reducing agents (Do Kim et al., 2004). As the content of *C. longa* powder increased up to 12.5 g.L⁻¹, the intensity of the absorption peak of obtained AgNPs solution decreased dramatically owing to the aggregation of AgNPs (Nagar et al., 2016). Moreover, the highest absorption peak was obtained at 10.0 g.L⁻¹ and selected as the suitable *C. longa* powder concentration in further experiments.

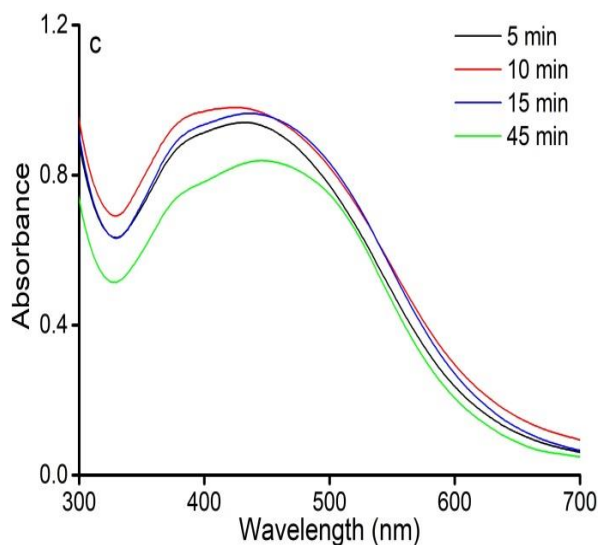
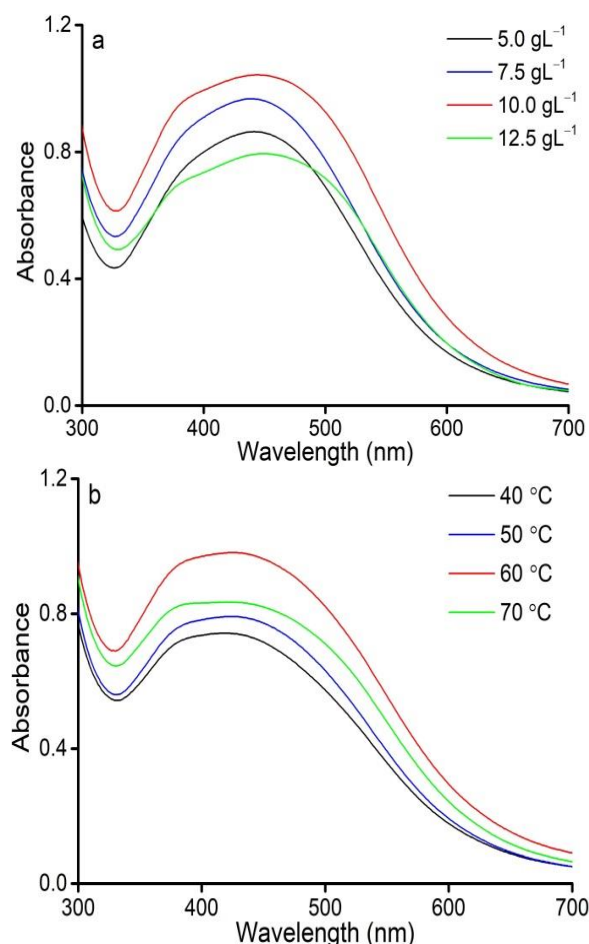


Figure 1: Effects of extraction conditions on AgNPs formation; (a) The *C. longa* raw material/water ratios; (b) The extraction temperature; (c) The extraction duration.

According to Figure 1b, the UV-Vis spectra determined the effect of extraction temperature on AgNPs synthesis by *C. longa* powder at AgNO₃ concentration of 1 mM, *C. longa* powder content of 10.0 g.L⁻¹, and the AgNO₃ solution (1.0 mM)/*C. longa* extract volume ratio of 2 at room temperature for 90 min. It was observed that an increase in intensity peak can be correlated with an enhancement in the extraction temperature of *C. longa* powder at the range of 40–60 °C. At the higher extraction temperature (70 °C), there was a remarkable decline for AgNPs formation. According to Rucha (Desai et al., 2012), AgNPs can be aggregated by undesired organic compounds in the extract at high extraction temperature. Therefore, 60 °C was selected as a suitable temperature for *C. longa* extraction.

Figure 1c shows the effect of the extraction duration of *C. longa* powder on the formation of AgNPs at different durations of 5, 10, 15, and 45 min at the AgNO₃ concentration of 1 mM, *C. longa* powder content of 10.0 g.L⁻¹, and the AgNO₃ solution (1.0 mM)/*C. longa* extract volume ratio of 2 at room temperature for 90 min. It could be observed that the absorption of the synthesized AgNPs solution increased with increasing the extraction duration from 5 to 10 min. As the extraction duration was prolonged (15 and 45 min), the intensity of AgNPs absorption decreased considerably, indicating that the desorption of biomolecules led to the reduced formation of AgNPs (Elemike et al., 2017). Thus, the suitable duration for the extraction of *C. longa* powder was 10 min.

In summary, the appropriate extraction parameters including the *C. longa* concentration of 10.0 g.L⁻¹, the extraction temperature of 60 °C, and the extraction duration of 10 min were concluded for further experiments.

Effects of synthesis conditions

The effects of synthesis conditions on the formation of AgNPs using *C. longa* extract are shown in Figure 2. The reactions were done at the volume ratio of the AgNO₃ solution (0.1 mM)/*C. longa* extract of 1, 2, 3, and 4, and varied concentrations of AgNO₃ in the range of 0.75, 1.00, 1.25, and 1.50 mM. Figure 2a shows the UV-Vis spectra of the synthesized AgNPs obtained at different mixing ratios of *C. longa* extract and the AgNO₃ solution. There was the presence of AgNPs at $V_{Ag^+}/V_{Ext} = 1$. On increasing V_{Ag^+}/V_{Ext} value of 2, AgNPs had the highest absorption peak and the absorption of synthesized AgNPs solution weakened at $V_{Ag^+}/V_{Ext} = 3$ and 4. When the extract volume was high, the AgNPs production reduced as a result of the dilution of AgNO₃ solution. Furthermore, the agglomeration of synthesized AgNPs occurred in the increased AgNO₃ volume (Prabhu and Poulouse, 2012).

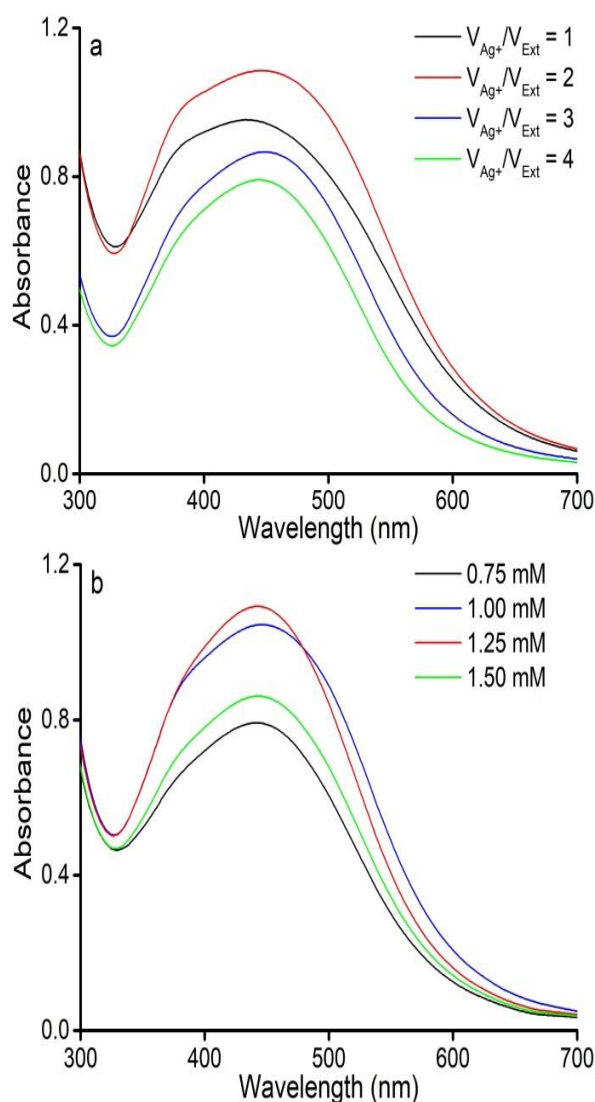


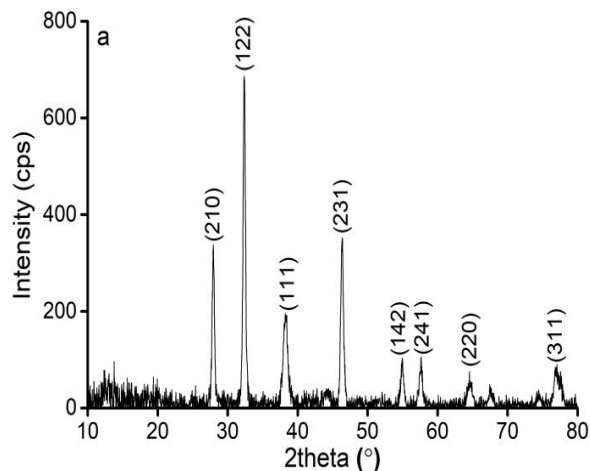
Figure 2: Effect of the conditions of AgNPs synthesis. (a) The volume ratios of AgNO₃ solution/*C. longa* extract. (b) AgNO₃ concentration.

Figure 2b indicates that the AgNO₃ concentration of 1.25 mM was suitable for the AgNPs synthesis. By a gradual increase in the concentration of AgNO₃ from 0.75 to 1.25 mM, the nanoparticle production increased. However, further increasing to 1.50 mM, led to the decreased absorption intensity of AgNPs. A higher concentration of AgNO₃ accelerated the reduction of Ag⁺ ions to AgNPs but at the same time, the deficiency of capping agents prevented from aggregation (Raman et al., 2015).

Characterization of AgNPs

The crystalline structure of AgNPs was determined by XRD. Figure 3a shows that the eight distinct diffraction peaks at 28.0, 32.4, 38.3, 46.3, 55.0, 57.6, 64.7, and 76.8° can be assigned for the (210), (122), (111), (231), (142), (241), (220), and (311) plane of Ag, respectively (Priyadharshini et al., 2014; Jemal et al., 2017). Based on the XRD results, the average crystal size of the sample at the (111) crystallographic plane was determined following Scherrer's equation (Patterson, 1939) with $K = 0.94$. The average size of the synthesized AgNPs reached 27.6 nm. Compared with previous studies (Mitiku and Yilma, 2018), the size of silver nanoparticles synthesized in this work using *C. longa* extract as a reducing agent was smaller than that of synthesized from *Artemisia Nilagirica* (70–90 nm), *Camellia Sinensis* (30–40 nm), *Acalypha Indica* (20–30 nm), *Cassia Fistula* (50–60 nm), *Boswellia ovali Foliolata* (30–40 nm), *Chenopodium murale* (30–50 nm), *Dioscorea bulbifera* (35–60 nm), *Cinnamomum Camphora* (55–80 nm), and *Eucalyptus Hybrid* (50–150 nm).

The elemental signals of AgNPs synthesized using *C. longa* extract were analyzed by EDX (see Figure 3b). The EDX spectrum determined the presence of C (44.47 wt.%), O (19.23 wt.%), F (4.54 wt.%), P (0.53 wt.%), Cl (11.93 wt.%), and Ag (19.31 wt.%) elements (Table 1). Peaks at 3.0, 3.2, and 3.4 keV were assigned to Ag (Jeeva et al., 2014). The weak signals of O, F, P, and Cl elements may be due to the biomolecules in the extract bound to the surface of the biosynthesized AgNPs (Kalathil et al., 2011). Moreover, the presence of the C signal was due to the sample preparation on a glass substrate. This result also confirmed the formation of AgNPs.



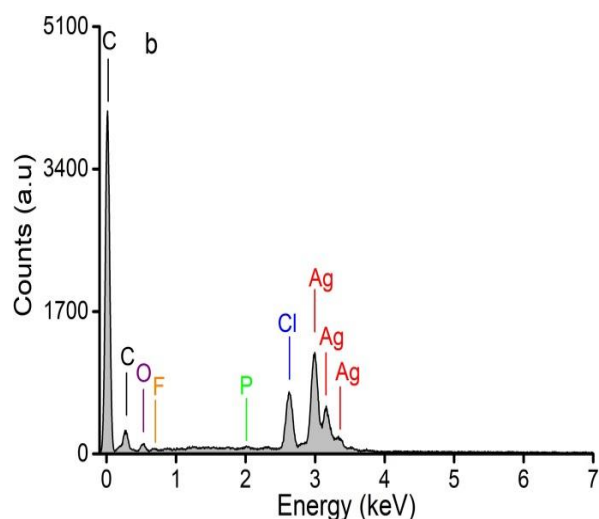


Figure 3: XRD pattern (a) and EDX spectrum (b) of synthesized AgNPs.

Table 1: The element composition forms the EDX spectrum.

Element	C	O	F	P	Cl	Ag
Atomic (wt.%)	44.47	19.23	4.54	0.53	11.93	19.31

The FTIR spectra were recorded to identify the biomolecules that were responsible for the reduction of the Ag^+ ions and capping of the reduced AgNPs synthesized by the *C. longa* extract (see Figure 4). The FTIR spectrum of *C. longa* extract showed peaks at 3423, 2926, 2860, 1640, 1316, and 1055 cm^{-1} . Correspondingly, the peaks of the synthesized AgNPs were at 3441, 2923, 2853, 1630, 1384, and 1045 cm^{-1} . A broad and strong band at 3441 cm^{-1} was due to O–H stretch of phenols. The peaks at around 2923 and 2853 cm^{-1} correspond to C–H stretch of aromatics and $-\text{OCH}_3$ groups. The band at 1630 cm^{-1} was owing to bond C=O bend and C=C stretch. A peak appeared at 1384 cm^{-1} indicates the binding of Ag to the C=O group of the curcumin and the band was observed at 1045 cm^{-1} corresponds to C–O stretching (Yang et al., 2016; Satyavani et al., 2011).

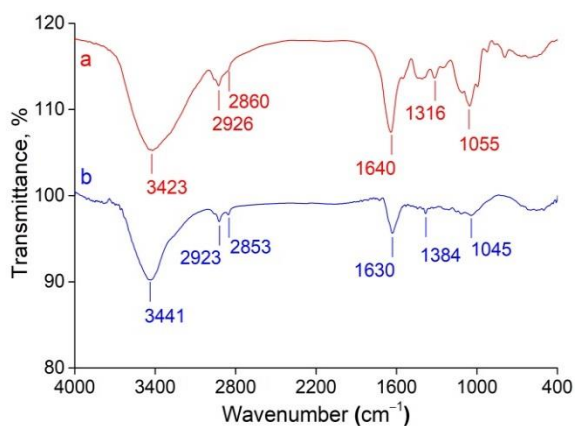


Figure 4: FTIR spectra of (a) *C. longa* extract and (b) synthesized AgNPs.

The result obtained from the TEM image clearly indicated the shape and size of AgNPs. Figure 5a shows that the synthesized AgNPs had spherical shapes in the diameter of 5 to 30 nm. Figure 5b shows the particle size histogram of AgNPs is shown in. The synthesized AgNPs possessed an average size of 28.0 nm. This result is consistent with the obtained XRD and TEM results.

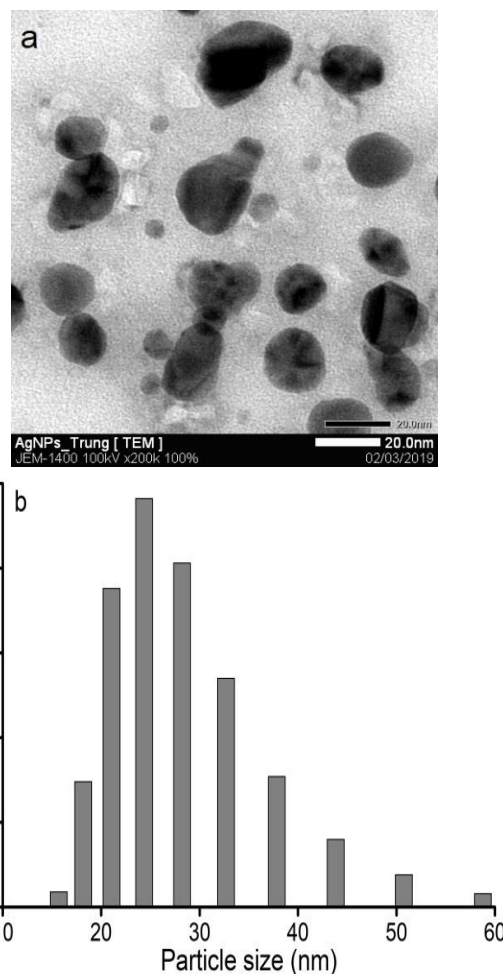


Figure 5: TEM image (a) and the particle size distribution histogram (b) of the biosynthesized AgNPs.

The mechanism for AgNPs formation

The major phytochemicals in *C. longa* powder were polyphenols. According to a study (Shishodia et al., 2007), the possible mechanism for the synthesis of AgNPs was also explained by $-\text{OH}$ groups of curcumin in the *C. longa* extract. These phytochemicals were as high reducing agents along with strong antioxidants for the reduction of Ag^+ ions to AgNPs. The reduction process was due to the electron-donating ability of phenol hydroxyl. Figure 6 demonstrates the mechanism for AgNPs formation using *C. longa* extract. Firstly, Ag^+ ions formed an intermediate complex with $-\text{OH}$ groups of curcumin and then oxidized curcumin into ketone form with the release of free electrons and Ag^+ ions. Next, these Ag^+ ions reduced to zero-

valent Ag. Finally, obtained AgNPs were stabilized by curcumin in the extract (Rao and Paria, 2013).

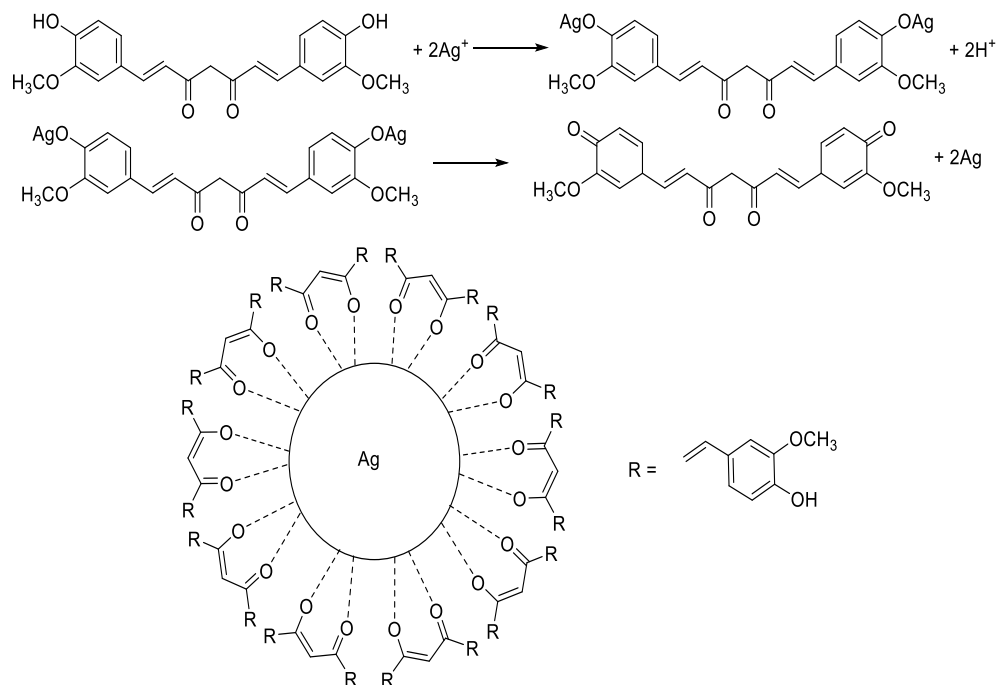
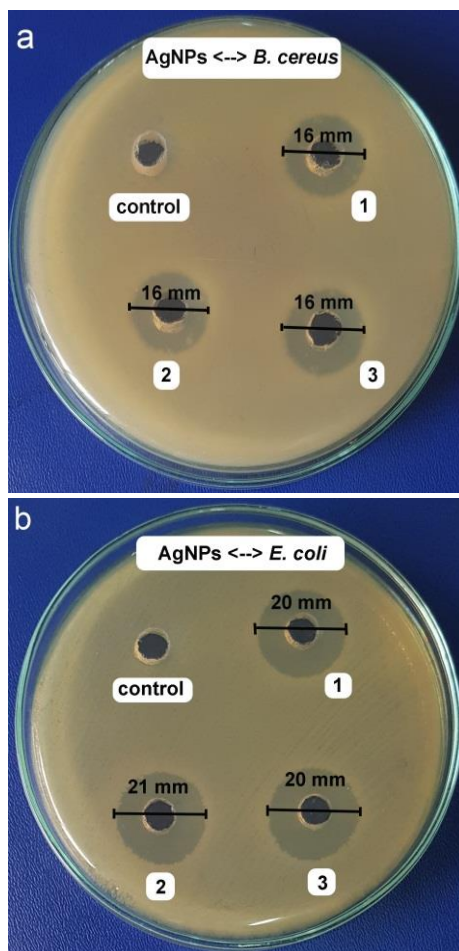


Figure 6: The mechanism for the formation of AgNPs using *C. longa* extract.

Antibacterial activity

The antibacterial effect of the biosynthesized AgNPs was analyzed against gram-negative bacteria (*E. coli* and *Salmonella*) and gram-positive bacteria (*S. aureus* and *B. cereus*). The obtained results (not shown) indicated that *C. longa* extract had no antibacterial effect against all bacteria including *Salmonella*, *E. coli*, *S. aureus*, and *B. cereus*. However, the AgNPs solution synthesized by *C. longa* extract had high antibacterial activity against these bacteria (see Figure 7). For gram-positive *S. aureus* and *B. cereus*, the average inhibition zone was 15 and 16 mm, respectively. Also, the zone of inhibition in diameter was 19 and 20 mm for *Salmonella* and *E. coli*, respectively. When comparing the zone of inhibition of AgNPs on the two microorganisms, the gram-negative bacteria inhibited better than gram-positive bacteria. According to Prakash (2013), the cell wall of gram-positive bacteria is constituted of a multiple layer of peptidoglycan forms, which are rigid structures. Thus, the synthesized AgNPs had a complicated diffusion and penetration to cause cell death. In some comparative studies on the synthesized AgNPs using the extract of *Astragalus gummifer* (Kora and Arunachalam, 2012), *Bhargavaea indica* (Singh et al., 2015), and *Ziziphus nummularia* (Khan et al., 2016), the results revealed that the AgNPs synthesized from *C. longa*, has stronger antibacterial effect than the mentioned extractions (Table 2



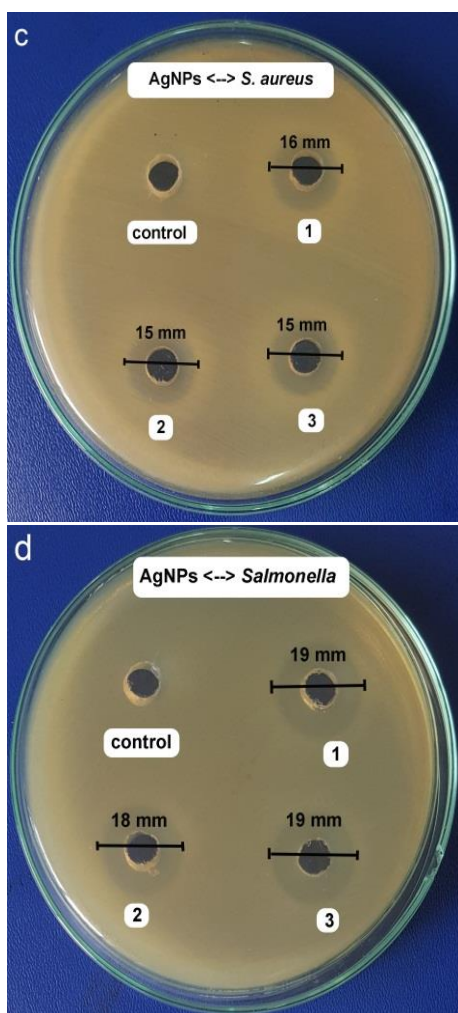


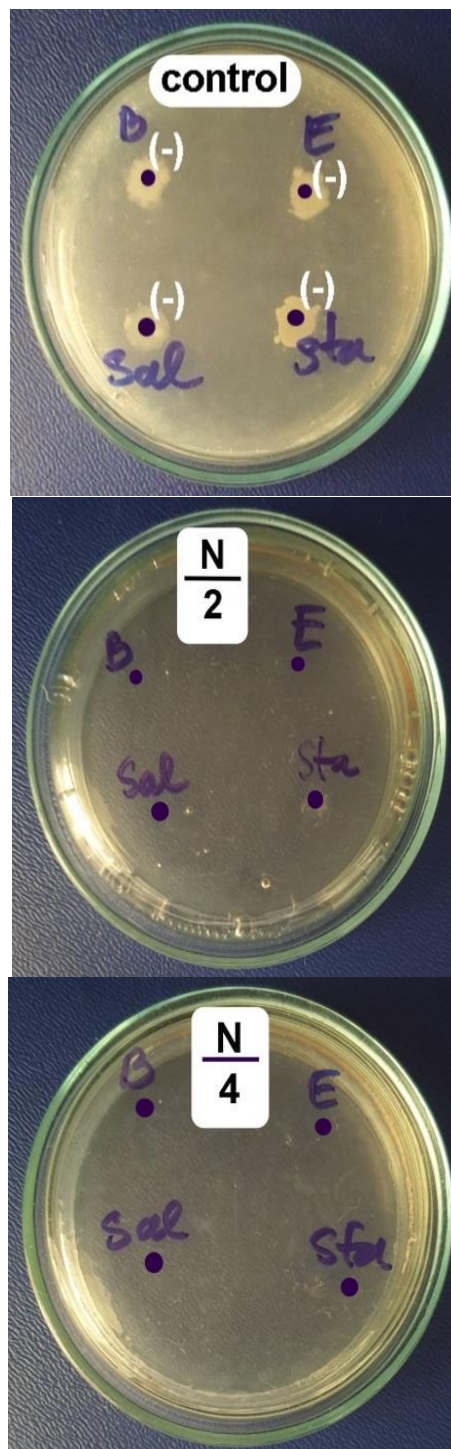
Figure 7: The inhibition zones caused by the synthesized AgNPs solution against *B. cereus* (a), *E. coli* (b), *S. aureus* (c), and *Salmonella* (d) at the most suitable conditions.

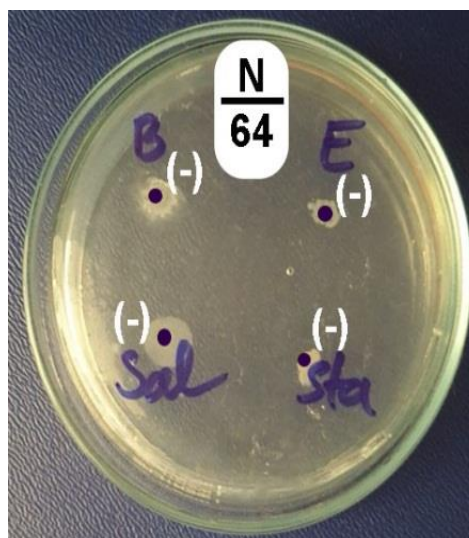
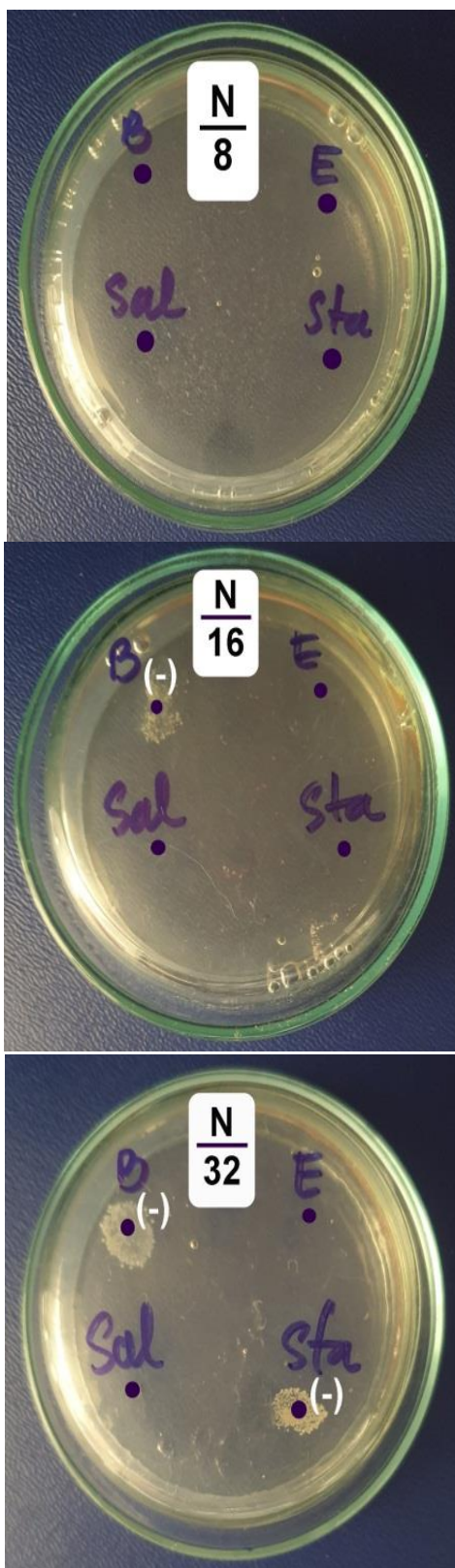
Table 2: The antibacterial activity of the tested aqueous extract of *C. longa* and the different plant extracts.

AgNPs from the different extracts	Inhibition zones (mm) observed with different bacteria				References
	<i>B. cereus</i>	<i>E. coli</i>	<i>S. aureus</i>	<i>Salmonella</i>	
<i>C. longa</i>	16	20	15	19	This work
<i>Astragalus gummifer</i>	12	10	–	–	Kora and Arunachalam, 2012
<i>Bhargavaea indica</i>	15	10	18	14	Singh et al., 2015
<i>Ziziphus nummularia</i>	16	18	18	21	Khan et al., 2016

Figure 8 presents the size of the inhibition zones induced by AgNPs solution against *B. cereus*, *E. coli*, *Salmonella*, and *S. aureus* with different concentrations. It was observed that the exponential phase of bacteria delayed in the presence of AgNPs

and this phenomenon was more obvious with the increase of AgNPs concentration. The MIC values of AgNPs samples against four bacteria are arranged in the order *Salmonella* = *E. coli* ($2.81 \mu\text{g.mL}^{-1}$) < *S. aureus* ($5.63 \mu\text{g.mL}^{-1}$) < *B. cereus* ($11.25 \mu\text{g.mL}^{-1}$). These obtained results showed that AgNPs can be used as effective growth inhibitors in five bacteria tested.





(-): Bacteria colonies were detected.

Figure 8: Images of the minimum inhibitory concentration of AgNPs samples against *E. coli* (E), *B. cereus* (B), *Salmonella* (Sal), and *S. aureus* (Sta).

Conclusions

The synthesis of AgNPs was successfully conducted using *C. longa* extract, in which curcumin performed the role of reducing, stabilizing, and capping agents for AgNPs formation. AgNPs were formed within the 90-minute reaction. The synthesized AgNPs were confirmed by XRD, EDX, and TEM analysis. The average size of the obtained AgNPs was 28.0 nm. Additionally, the biosynthesized AgNPs had antibacterial activity against the gram-negative bacteria (*Salmonella* and *E. coli*) and the gram-positive bacteria (*S. aureus* and *B. cereus*) by disc diffusion method with the zone inhibition and the MIC on the agar plate. These results showed that the obtained AgNPs using *C. longa* extract could be useful for the development of newer and more effective antibacterial agents for health care.

Acknowledgments

This research is funded by Can Tho University under grant number T2019-84.

References

- Abraham A, Samuel S, & Mathew L. (2018). Pharmacognostic Evaluation of *Curcuma longa* L. Rhizome and Standardization of its Formulation by HPLC Using Curcumin as Marker. *International Journal of Pharmacognosy and Phytochemical Research*, 10(1), 38-42.
- Desai, R., Mankad, V., Gupta, S. K., & Jha, P. K. (2012). Size distribution of silver nanoparticles: UV-visible spectroscopic assessment. *Nanoscience and Nanotechnology Letters*, 4(1), 30-34.

- Do Kim, K., Han, D. N., & Kim, H. T. (2004). Optimization of experimental conditions based on the Taguchi robust design for the formation of nano-sized silver particles by chemical reduction method. *Chemical Engineering Journal*, 104(1-3), 55-61.
- Elemike, E. E., Onwudiwe, D. C., Arijeh, O., & Nwankwo, H. U. (2017). Plant-mediated biosynthesis of silver nanoparticles by leaf extracts of *Lasienthra africanum* and a study of the influence of kinetic parameters. *Bulletin of Materials Science*, 40(1), 129-137.
- Garg, S., & Garg, A. (2018). Encapsulation of curcumin in silver nanoparticle for enhancement of anticancer drug delivery. *Int J Pharm Sci Res*, 9, 1160-1166.
- Gittins, D. I., Bethell, D., Schiffrin, D. J., & Nichols, R. J. (2000). A nanometre-scale electronic switch consisting of a metal cluster and redox-addressable groups. *Nature*, 408(6808), 67-69.
- Janeeta Priya, F., Rosaline Vimala, J., Sathya Bama, R., & Lavanya, M. (2016). Green Synthesis of silver nanoparticles using aqueous extract of *ficus racemosa* bark and its antimicrobial activity. *World Journal of Pharmacy and Pharmaceutical Sciences*, 5, 753-65.
- Jeeva, K., Thiagarajan, M., Elangovan, V., Geetha, N., & Venkatachalam, P. (2014). *Caesalpinia coriaria* leaf extracts mediated biosynthesis of metallic silver nanoparticles and their antibacterial activity against clinically isolated pathogens. *Industrial Crops and Products*, 52, 714-720.
- Jemal, K., Sandeep, B. V., & Pola, S. (2017). Synthesis, characterization, and evaluation of the antibacterial activity of *Allophylus serratus* leaf and leaf derived callus extracts mediated silver nanoparticles. *Journal of Nanomaterials*, 2017.
- Kalathil, S., Lee, J., & Cho, M. H. (2011). Electrochemically active biofilm-mediated synthesis of silver nanoparticles in water. *Green Chemistry*, 13(6), 1482-1485.
- Khan, F. A., Zahoor, M., Jalal, A., & Rahman, A. U. (2016). Green synthesis of silver nanoparticles by using *Ziziphus nummularia* leaves aqueous extract and their biological activities. *Journal of Nanomaterials*, 2016.
- Kora, A. J., & Arunachalam, J. (2012). Green fabrication of silver nanoparticles by gum tragacanth (*Astragalus gummifer*): a dual functional reductant and stabilizer. *Journal of Nanomaterials*, 2012.
- Kriithiga, J., & Briget, M. M. (2015). Synthesis of AgNPs of *Momordica charantia* leaf extract, characterization and antimicrobial activity. *Pharm Anal Acta*, 6, 427.
- Kurian, M., Varghese, B., Athira, T. S., & Krishna, S. (2016). Novel and efficient synthesis of silver nanoparticles using *curcuma longa* and *zingiber officinale* rhizome extracts. *International Journal of nanoscience and nanotechnology*, 12(3), 175-181.
- Manonmani, P., Ramar, M., Geetha, N., Arasu, M. V., Erusan, R. R., Mariselvam, R., & Sowmiya, J. J. (2015). Synthesis of silver nanoparticles using natural products from *Acalypha indica* (Kuppaimeni) and *Curcuma longa* (turmeric) on antimicrobial activities. *IJPRBS*, 4, 151-64.
- Mitiku, A. A., & Yilma, B. (2018). A review on green synthesis and antibacterial activity of silver nanoparticles. *Int. J. Pharm. Sci. Rev. Res*, 46, 52-57.
- Mukherjee, 4., Roy, M., Mandal, B. P., Dey, G. K., Mukherjee, P. K., Ghatak, J., ... & Kale, S. P. (2008). Green synthesis of highly stabilized nanocrystalline silver particles by a non-pathogenic and agriculturally important fungus *T. asperellum*. *Nanotechnology*, 19(7), 075103.
- Nagar, N., Jain, S., Kachhawah, P., & Devra, V. (2016). Synthesis and characterization of silver nanoparticles via green route. *Korean Journal of Chemical Engineering*, 33(10), 2990-2997.
- PANDIT, R. (2015). Green synthesis of silver nanoparticles from seed extract of *Brassica nigra* and its antibacterial activity. *Nusantara Bioscience*, 7(1).
- Patil, B. S., Jayaprakasha, G. K., Chidambara Murthy, K. N., & Vikram, A. (2009). Bioactive compounds: historical perspectives, opportunities, and challenges. *Journal of agricultural and food chemistry*, 57(18), 8142-8160.
- Patterson, A. L. (1939). The Scherrer formula for X-ray particle size determination. *Physical review*, 56(10), 978.
- Prabhu, S., & Poulouse, E. K. (2012). Silver nanoparticles: mechanism of antimicrobial action, synthesis, medical applications, and toxicity effects. *International nano letters*, 2(1), 32.
- Prakash, P., Gnanaprakasam, P., Emmanuel, R., Arokiyaraj, S., & Saravanan, M. (2013). Green synthesis of silver nanoparticles from leaf extract of *Mimusops elengi*, Linn. for enhanced antibacterial activity against multi drug resistant clinical isolates. *Colloids and Surfaces B: Biointerfaces*, 108, 255-259.
- Prasad, S., Gupta, S. C., Tyagi, A. K., & Aggarwal, B. B. (2014). Curcumin, a component of golden spice: from bedside to bench and back. *Biotechnology advances*, 32(6), 1053-1064.
- Priyadarshini, R. I., Prasannaraj, G., Geetha, N., & Venkatachalam, P. (2014). Microwave-mediated extracellular synthesis of metallic silver and zinc oxide nanoparticles using macro-algae (*Gracilaria edulis*) extracts and its anticancer activity against human PC3 cell lines. *Applied biochemistry and biotechnology*, 174(8), 2777-2790.
- Raman, R. P., Parthiban, S., Srinithya, B., Kumar, V. V., Anthony, S. P., Sivasubramanian, A., & Muthuraman, M. S. (2015). Biogenic silver nanoparticles synthesis using the extract of the medicinal plant *Clerodendron serratum* and its in-vitro antiproliferative activity. *Materials Letters*, 160, 400-403.
- Rao, K. J., & Paria, S. (2013). Green synthesis of silver nanoparticles from aqueous *Aegle marmelos* leaf extract. *Materials Research Bulletin*, 48(2), 628-634.
- Sandeep, S., Santhosh, A. S., Swamy, N. K., Suresh, G. S., Melo, J. S., & Mallu, P. (2016). Biosynthesis of silver nanoparticles using *Convolvulus pluricaulis* leaf extract and assessment of their catalytic, electrocatalytic and phenol remediation properties. *Adv. Mater. Lett*, 7(5), 383-389.
- Sathishkumar, M., Sneha, K., & Yun, Y. S. (2010). Immobilization of silver nanoparticles synthesized using *Curcuma longa* tuber powder and extract on cotton cloth for

- bactericidal activity. *Bioresource technology*, 101(20), 7958-7965.
- Satyavani, K., Ramanathan, T., & Gurudeeban, S. (2011). Green synthesis of silver nanoparticles by using stem derived callus extract of bitter apple (*Citrullus colocynthis*). *Dig J Nanomater Biostruct*, 6(3), 1019-1024.
- Shameli, K., Ahmad, M. B., Zamanian, A., Sangpour, P., Shabanzadeh, P., Abdollahi, Y., & Zargar, M. (2012). Green biosynthesis of silver nanoparticles using *Curcuma longa* tuber powder. *International journal of nanomedicine*, 7, 5603.
- Shehzad, A., Rehman, G., & Lee, Y. S. (2013). Curcumin in inflammatory diseases. *Biofactors*, 39(1), 69-77.
- Shishodia, S., Chaturvedi, M. M., & Aggarwal, B. B. (2007). Role of curcumin in cancer therapy. *Current problems in cancer*, 31(4), 243-305.
- Singh, P., Kim, Y. J., Singh, H., Mathiyalagan, R., Wang, C., & Yang, D. C. (2015). Biosynthesis of anisotropic silver nanoparticles by *Bhargavaea indica* and their synergistic effect with antibiotics against pathogenic microorganisms. *Journal of Nanomaterials*, 2015.
- Yang, X. X., Li, C. M., & Huang, C. Z. (2016). Curcumin modified silver nanoparticles for highly efficient inhibition of respiratory syncytial virus infection. *Nanoscale*, 8(5), 3040-3048.